Modelling the Elastic Properties of Balloons as Substitutes for Exosomes

Olga Borbély
olga.agnes.borbely@gmail.com

under the direction of
Assistant Prof. Dhrubaditya Mitra
Nordic Institute for Theoretical Physics

Research Academy for Young Scientists
July 14, 2021

Abstract

Exosomes, the intercellular information transmitters in eukaryotes, have potential in hormone therapy and cancer diagnostics and are thus of great interest in current research. Information about the protein profiles of exosomes can be used to trace tumors and infections, as the protein profiles are determined by the cells that the exosomes are secreted by. Previous studies have found a correlation between the protein profiles of exosomes and their elasticity. It is therefore of importance to determine the elastic properties of exosomes. This usually takes the form of analysis of the data from atomic force microscopes, using the Hertz model.

The aim of this study was to provide a general understanding of the elastic properties of spherical objects under pressure, to determine whether or not balloons would be suitable models of exosomes and to discuss the reliability of the Hertz model. This was examined through measurements on different balloons. A linear relationship between the compressing force on the balloon and its displacement was found. Furthermore, the spring constant of a balloon was found to be dependent on the internal pressure and the shape of the tip that it was indented by. The conclusion drawn was that balloons and exosomes differ in terms of the relation between the compressing force and the displacement. Future research may, however, be needed to investigate further potential similarities between exosomes and balloons.

Acknowledgements

I would like to express my deepest gratitude to Assistant Professor Dhrubaditya Mitra at Nordic Institute for Theoretical Physics, whose expertise, guidance and great mentorship have been of utmost importance for this project. I also wish to thank Ph.D. students Sara Cavallaro and Moein Talebian Gevari, whose practicality, patience and reassuring presence in the laboratory were of great help. Many great thanks goes to Prof. Apurba Dev for providing his knowledge and guidance during this project. A special thanks should be given to Tomas Eneroth at the Albanova Workshop, whose expertise and skills were crucial for this research and to Fredrik Stridfeldt at Nordic Institute for Theoretical Physics for always opening new doors. I wish to thank all the xRays who offered their time and provided me with helpful feedback. I would furthermore like to extend my thanks to my colleague Tilde Berglind for her cooperation. Finally, I would like to offer my special thanks to Max Kenning, Markus Swift, Ann-Kristin Malz and Miranda Carlsson, the organizers of Research Academy for Young Scientists and their collaborative partners Kjell & Märta Beijers Stiftelse and AstraZeneca for making this project possible.

Contents

1 Introduction

Exosomes are vesicles secreted by cells via exocytosis which can be found in biofluids such as urine, blood, and saliva in mammals [1]. During exocytosis, exosomes are formed by inward budding and scission of vesicles from the adjacent endosomal membranes. As exosomes accumulate, intracellular sacs are created around them, see Figure 1a. The sacks than fuse with the cell membrane, the exosomes are released into biofluids and enabled to be taken up by other cells, see Figures 1b and 1c. [2]

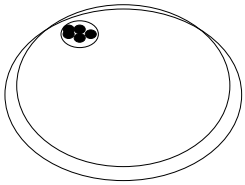

(a) An intracellular sack containing exosomes is created.

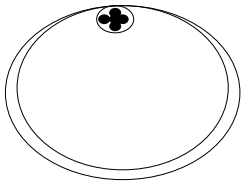

(b) The sack fuses with the cell membrane.

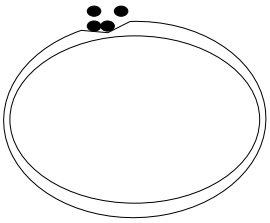

(c) The exosomes are secreted by the cell.

Figure 1: Exocytosis.

The presence of exosomes is required in numerous biological processes. One example is antigen presentation, where antigens are broken down by exosomes, allowing T-cells to recognize them and trigger an immune response. Other instances are transportation of mRNA or infectious agents and intercellular communication. [1]

Exosomes are essential to intercellular communication and substance transmission and can as such give rise to a change in cell behaviour and function in the body. Exosomes are therefore involved in the development of a number of disorders such as cancer, neurodegeneration and inflammatory diseases. [3]

Consequently, the detection of single receptor molecules on exosomes bearing characteristics of infections and diseases enables early diagnosis of maladies such as cancer. A further possible area of utilization is hormone therapy, as exosomes can be used to mimic drug delivery systems. [1]

Previous studies suggest that the exosome elasticity is influenced by the protein profiles of the exosomes. During an infection, the exosomes are marked with different proteins than their characteristic ones [4]. Determining the connection between the protein profiles of exosomes is therefore of interest, as it could be used in diagnostics and for medical treatments.

Previous studies have shown that different types of deformability can be observed depending on the type of measurement. The values of the elasticity-characterizing quantities vary from report to report, suggesting differences in how the results of different methods are obtained or analyzed. [5]

A change in the morphology of exosomes determined by the loading force acting on them can be observed in many cases. Indentation in the middle of the vesicle and an increase of its lateral dimensions are the results of a greater loading force. When put under low stress, exosomes possess the ability to regain their original form after deforming, i.e. their properties are elastic. However, the effects of greater stress are permanent deformation and eventual disintegration. [1]

As exosome elasticity and deformability vary depending on the circumstances, it is of interest to obtain a general understanding of these quantities.

1.1 Atomic Force Microscopy

A common way of examining the elastic properties of exosomes is using atomic force microscopes (AFM), see Figure 2 [6]. The AFM uses piezoelectric crystals in order to determine the force that is exerted by the cantilever tip on the sample [6]. These are crystals made up of materials such as ZnO, GaN and InN and have a non-central sym-

metry. When stress is applied to the piezoelectric crystals, an electric potential is created due to the polarization of the ions [7]. The measurement of this potential enables the determination of the magnitude of the force acting on the crystals, which corresponds to the magnitude of the force exerted by the cantilever on the sample [8].

The size of a pixel being indented by the cantilever tip can be adjusted before the scanning. A pixel is indented once during one scan. Since the exosomes in the sample are in a solution, a number of scans might be necessary to localize them and adjust the pixel size so that the surface of an exosome is indented by the cantilever tip in various points. [9]

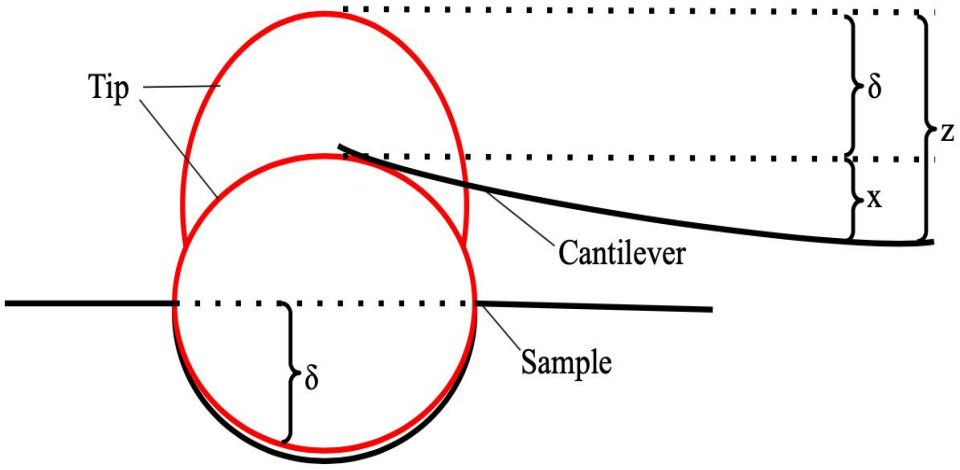

Figure 2: The measurements are done by the AFM as follows: a cantilever is let down by a distance z so that its tip (represented by the circle) touches the sample. When in contact with the sample, the cantilever is bent upwards, moving up by a distance x. Consequently, the sample is indented by the distance $\delta = z - x$.

In the AFM, a laser beam is reflected by the cantilever and received by a photodetector, see Figure 3 [10]. The intensity of the light reaching the photodetector depends on the amount of light that is reflected towards it. That is determined by the tilting of the cantilever which is dependent on its interaction with the sample. Consequently, the indentation δ of the sample can be determined by the intensity of the laser light received by the photodetector. [11]

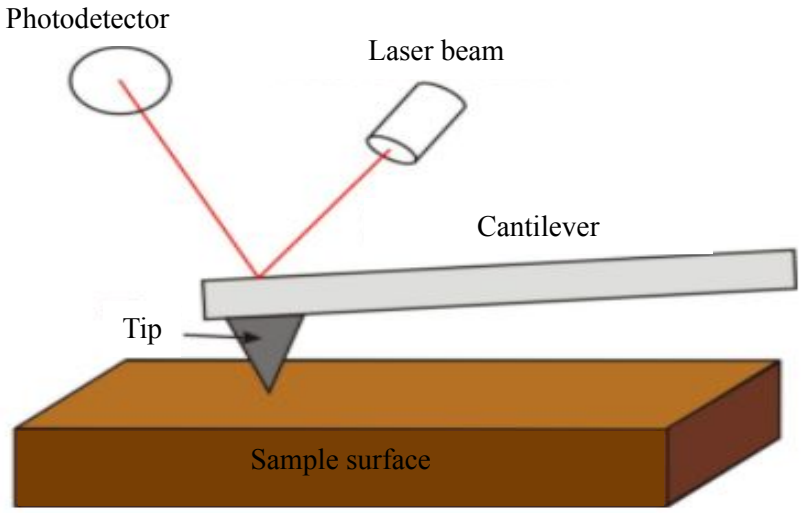

Figure 3: A laser beam reflected by the cantilever in an atomic force microscope.

Information about both the force exerted on the sample and its indentation is collected by the AFM. Consequently, an image of the sample determined by its topography is created. Additionally, this imaging technique allows for analysis of the data by plotting the force exerted on the sample as a function of its indentation for each area unit that is examined. From such plots, the elastic properties of the sample can be calculated. [6]

1.2 The Hertz Model

In order to describe the elastic properties of a body, the definition of the quantities stress and strain is essential. The stress τ on a body is defined as $\tau = \frac{F}{A}$ for a tensile or compressive force F acting on a cross sectional area A of the body perpendicular to F, and the corresponding strain ϵ is given by $\epsilon = \frac{\Delta l}{l}$ in which Δl is the resulting deformation of the original length l of the object. A material-specific constant that relates τ to ϵ is the Young's modulus, Y that is defined as $Y = \frac{\tau}{\epsilon}$. [12]

For e.g. a solid block, τ and ϵ are easily measured or calculated. For spherical, partially viscous bodies such as exosomes, however, determining τ, ϵ and Y is more complicated. The Hertz model — that gives a relation between the force F acting on a sample in an

AFM and the indentation δ of the sample — can be used in such cases. This relation is dependent on the shape of the cantilever tip. For a parabolic tip, the Hertz model gives

$$F = \frac{4\sqrt{R}}{3}\frac{Y}{1-\sigma^2}\delta^{\frac{3}{2}} \tag{1}$$

in which R is the radius of the tip curvature as seen in Figure 4 [6], Y is the Young's modulus of the sample and σ is the Poisson's ratio, another material-specific constant that describes the elasticity of a material, of the sample [6].

Figure 4: The radius of the tip curvature, R.

For a conical tip, the Hertz model gives

$$F = \frac{Y}{1-\sigma^2}\frac{2\tan\alpha}{\pi}\delta^2 \tag{2}$$

in which α is the semi-opening angle of the cone as seen in Figure 5 [6].

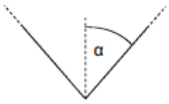

Figure 5: The semi-opening angle of a conical tip.

With the help of this model and the force-indentation plots obtained with the AFM measurements, the Y of the sample can be calculated given that R and α for the tips used and the σ of the sample are known. [6]

However, the Hertz model has some disadvantages when it comes to determining the elastic properties of biological samples. For one, the model assumes elastic behavior of the bodies involved [6]. The elastic properties of a material can be absolutely elastic or absolutely viscous. Absolutely elastic materials deform instantaneously to the equilibrium value of the strain when put under creep (non-dynamic) stress. This strain stands

in proportion to the applied force. In viscous fluids however, the flow of the fluid that occurs due to creep stress is indefinite and the velocity of the deformation is dependent on the viscosity — a material-specific quantity. [5]

As opposed to the assumptions made by the model, the elastic properties of most materials, including biological samples, are a mixture of absolute elasticity and absolute viscosity. Another assumption in the model is homogeneity of the material, whereas exosomes are not completely homogeneous [6].

Some of the assumptions made by the Hertz model are accounted for during AFM data analysis [6]. Additionally, AFM data from previous studies show that the relation between the compressing force on the exosomes and their displacement is non-linear [5]. However, it is of relevance to ask whether or not a different approach than the Hertz model offers more reliability when it comes to the determination of the exosome elasticity.

1.3 Aim of Study

In order to mimic the stress that is applied on the exosomes during an AFM scan and to provide a general understanding of how objects encased in an elastic shell act when affected by a compressive stress, measurements can be made on balloons. Thus, the purpose of this study was to examine the elastic properties of balloons, to determine whether or not balloons could be a suitable model of exosomes and whether or not there exist models that describe the elastic properties of different objects more accurately than the Hertz model does.

1.4 A System of Two Springs

According to Hooke's law, the relation between the magnitude of the compressing force F acting on a solid, elastic body and the compression Δl of the body is

$$F = -k\Delta l \tag{3}$$

where k is the spring constant of the body [13].

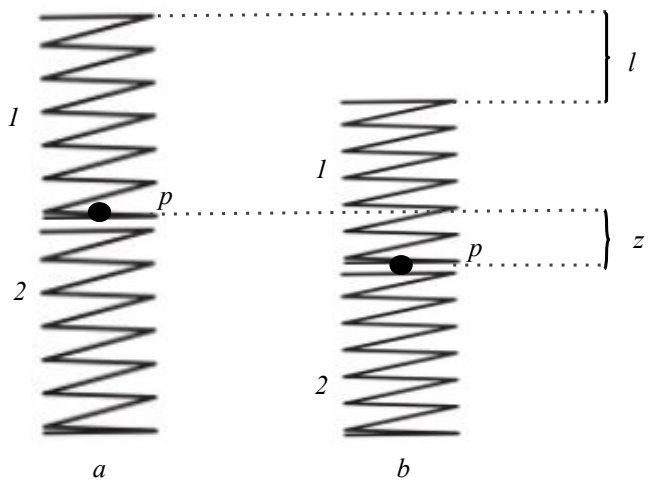

Figure 6: A system of two springs in two different states.

Figure 6 shows a system of two springs, 1 and 2 in two different states, a and b. In b, the system has been compressed with a length l, resulting in displacement of the point p by the length z. The change in length of spring 1 is given by $z - l$, and that of spring 2 is given by $-z$. If the compressing force on spring 1 is F, the restoring forces coming from springs 1 and 2 are also of magnitude F according to Newton's third law [14]. Equation (3) implies that

$$F = -k(z - l) \tag{4}$$

in which k is the spring constant of spring 1.

This can be applied on a system made up of a tip moved by a spring and a balloon indented by this tip. The relation between the compressing force F acting on the balloon and its displacement z may not be linear and could be better described by

$$F = k'z^d \iff \log(F) = \log(k') + d \cdot \log(z) \tag{5}$$

in which d and k' are constants and k' can be called the effective spring constant of the balloon.

If measurements on a system made up of a spring and a balloon are done so that l, $F(z)$ and k are either directly measured or calculated, it is possible to determine the value of z for a certain F. In that way, F can be plotted as a function of z and the nature of the relation between these quantities, i.e. the values of k' and d can be determined. Furthermore, the relation between z and F can be compared to the relation between these quantities for exosomes examined in AFM. This can be done by the comparison of the relation between $\frac{F}{F_{\max}}$ and $\frac{z}{z_{\max}}$ for AFM data and data obtained with experiments done on balloons, where F is the compressing force acting on an exosome or a balloon, $F_{\max}$ is the maximal compressing force applied during a measurement, z is the displacement of an exosome or a balloon, and $z_{\max}$ is the maximal displacement observed during a measurement.

1.5 Propagation of Error

The error in a quantity x that is dependent on the quantities a, b and c can be calculated according to

$$\sigma_x = \sqrt{(\frac{\partial x}{\partial a})^2\sigma_a^2 + (\frac{\partial x}{\partial b})^2\sigma_b^2 + (\frac{\partial x}{\partial c})^2\sigma_c^2} \tag{6}$$

in which σ_x, σ_a, σ_b and σ_c are the errors in the measurements of the quantities x, a, b and c respectively. [15]

2 Method

Measurements on balloons bought from a local convenience store were made and complemented with the determination of the spring constant of the spring used.

2.1 Measurements on the Balloons

The measurements were made using the setup shown in Figure 7. The balloon was placed on a scale with a precision of 1 g. A rod was attached to the table on which the scale stood and a platform was attached to the rod. A reading of the displacement of this platform could be noted from an arm, which measured the displacement up to 0.01 mm precision. A shorter rod was attached to the platform and a pipe, inside of which was a spring pushing on a tip, was attached to this rod. The movement of the platform was directly translated into a compression of the spring, resulting in the tip indenting the balloon. Initially, the tip barely touched the balloon, enabling the spring in the pipe to maintain its original form. The platform was then successively lowered at intervals of 0.5 mm and the reading on the scale was noted. This was repeated until the platform had been lowered 26 mm in total. This process was repeated twice with the same balloon.

Measurements were taken with different tips and at different internal balloon pressures ranging from 1.25 to 2 atm, see Table 1 and Figure 8. Before changing tips, the contact point for the tip and the balloon was marked and the setup reconstructed so that the tip touched the balloon in the same point as previously.

Based on the data obtained with these measurements, the force F acting on the balloon could be calculated according to $F = mg$, in which m is the mass measured by the scale and g is the gravitational acceleration in $\mathrm{m\,s^{-2}}$. Since the compression of the whole system l was measured, the compression of the balloon z could be calculated according to Equation (4).

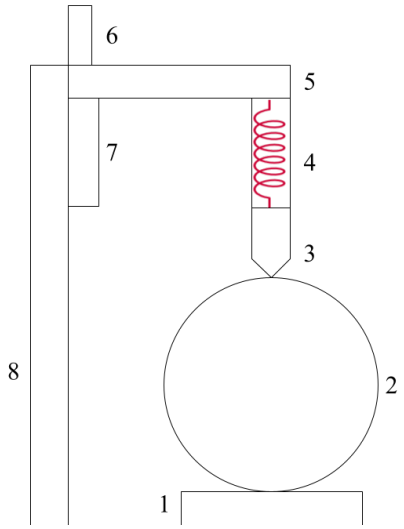

Figure 7: Schematic figure of the setup used for the measurements on the balloon. 1: Scale, 2: Balloon, 3: Tip, 4: Spring inside the pipe, 5: Shorter rod, 6: Arm of platform where the reading can be noted, 7: Platform, 8: Rod attached to the table.

Table 1: An overview of the different measurements made using method 2.

Measurement	Internal Pressure of the Balloon ± 0.0005 atm	Balloon	Shape of Tip
1	2 atm	1	dull
2	2 atm	1	sharp
3	1.5 atm	2	dull
4	1.5 atm	2	sharp
5	1.25 atm	3	dull
6	1.25 atm	3	sharp

Figure 8: The tips used in the measurements on the balloon. The sharp tip on the left and the dull one on the right.

A linear plot as well as a logarithmic plot for F as a function of z, each with a corresponding linear fit, were plotted with the method of least squares. The R^2-values of these regressions were calculated and the errors for the slopes were derived using Equation (6). Additionally, $\frac{F}{F_{\max}}$ was plotted as a function of $\frac{z}{z_{\max}}$.

2.2 Measurement of the Spring Constant of the Spring

The balloon was removed from the setup used previously, and the spring turned upside-down before it was placed back into the pipe, so that the flat end was the one in the lower end of the pipe. Then, the platform was lowered so that the flat end of the tip barely touched the scale, enabling the spring to maintain its original form (see Figure 9). The platform was successively lowered at intervals of 1 mm, compressing the spring. The reading on the scale was noted for each time. This was repeated until it had been lowered 6 mm in total. The process was repeated twice.

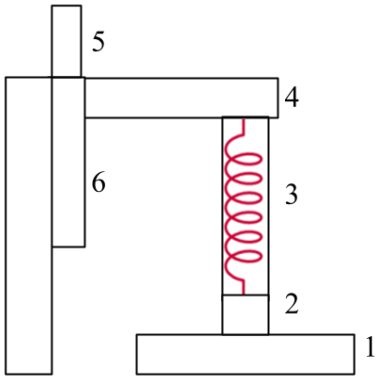

Figure 9: A schematic figure of the setup used for the measurement of the spring constant of the spring. 1: Scale, 2: Tip turned around so that its flat side is in contact with the scale, 3: Spring inside the pipe, 4: Shorter rod, 5: Arm of platform where the reading can be noted, 6: Platform.

A regression for F as a function of the displacement of the spring x (corresponding to the reading on the arm of the platform) was plotted. The fit was made with the method of least squares and its R^2-value was calculated. The error for the slope of this line was

calculated using Equation (6).

3 Results

Based on the regression obtained using the data from the measurements on the spring, see Figure 10 in Appendix A, the spring constant k of the spring was found to be $3100\,\mathrm{N\,m^{-1}}$, the R^2-value of the regression was found to be 0.968, and the potential error span in the spring constant was found to be $\pm 5.68\,\mathrm{N\,m^{-1}}$.

The logarithmic plot and the linear regression of F as a function of z gave rise to the lines presented in Figures 11 and 12 in Appendix B. For the slopes of the fitted lines, the R^2-values of the regressions and the errors for the slopes, see Tables 2 and 3. The plot of $\frac{F}{F_{\max}}$ as a function of $\frac{z}{z_{\max}}$ yielded the lines in Figure 13 in Appendix B.

Table 2: An overview of the attributes of the logarithmic plot.

Measurement	Slope of Logarithmic Plot Line	R^2-value of Logarithmic Plot Regression
1	1.07	1.00
2	1.10	0.982
3	1.07	0.992
4	1.12	0.970
5	1.08	0.995
6	1.08	0.933

Table 3: An overview of the attributes of the linear plot.

Measurement	Slope of Linear Plot Line [$\mathrm{N\,m^{-1}}$]	R^2-value of Linear Plot Regression	Error for Slope of Line [$\mathrm{N\,m^{-1}}$]
1	-156	0.998	± 0.794
2	-142	0.997	± 0.802
3	-143	0.998	± 0.798
4	-138	0.997	± 0.806
5	-148	0.998	± 0.798
6	-127	0.996	± 0.806

4 Discussion

Based on the data, the relation between the compressing force F on a balloon and the displacement z of the balloon could be determined. Derived from this relation, the elastic properties of a balloon could be compared with those of exosomes.

4.1 Determining the Exponent d in the Proportional Relation between F and z^d

The compressing force acting on an AFM sample is proportional to the displacement of the sample to the power of $\frac{3}{2}$ (parabolic tip) or 2 (conical tip) according to the Hertz model. In order to determine if this relation is linear in the case of the balloon, the lines obtained with the logarithmic plot of F as a function of z were used, as the slopes of those lines should correspond to d according to Equation (5). The slopes of the logarithmic plot lines presented in Table 2 and the R^2-values of the regressions are all roughly equal to 1. The relation between F and z is thus linear, and the spring constants k' of the different balloons can be determined by the slopes of the lines presented in Table 3, as these should correspond to $-k'$ according to Equation (3). The deviance from origo on the y-axis can be neglected. For an overview of the calculated spring constants and their errors, see Table 4.

Table 4: An overview of the calculated spring constants for the balloons used in the different measurements.

Measurement	Spring Constant of the Balloon $\mathrm{N\,m^{-1}}$	Error for the Spring Constant $\mathrm{N\,m^{-1}}$
1	156	± 0.796
2	142	± 0.802
3	143	± 0.798
4	138	± 0.806
5	148	± 0.798
6	127	± 0.806

4.2 Conclusion

In conclusion, indentation with the sharper tip gave rise to a spring constant up to $21\,\mathrm{N\,m^{-1}}$ lower than indentation with the duller one. This difference is significantly higher than the errors for the spring constants. However, this value can vary depending on where on its surface the balloon is poked. Furthermore, a balloon with lower internal pressure is found to have a lower spring constant. These differences are also significantly higher than the errors. However, an exception to this is the balloon used in measurement 5, which is believed to be an effect of random errors.

Conclusively, the Hertz model does not accurately describe balloons, since there is a linear relation between the compressing force acting on the balloon and the displacement of the balloon. Previous studies make it clear that this relation is non-linear for exosomes. However, the Hertz model assumes that the morphological changes of a sample caused by the AFM tip are local whereas the pressure inside of a balloon is uniform and the changes are communicated all over its surface and within. It is left for future research to determine whether or not exosomes share more similarities with balloons in this sense and whether or not a different model should be applied. It is also relevant to examine if there are materials that are similar to exosomes that could be used to mimic them on a bigger scale in order to supply a model for the calculation of their elastic properties. A good candidate for such an experiment would be hydrogel, since it is more viscous and does possibly share more similarities with exosomes.

References

[1] Sharma S, Rasool HI, Palanisamy V, Mathisen C, Schmidt M, Wong DT, et al. Structural-mechanical characterization of nanoparticle exosomes in human saliva, using correlative AFM, FESEM, and force spectroscopy. ACS nano. 2010;4(4):1921–1926.

[2] Simpson RJ, Jensen SS, Lim JW. Proteomic profiling of exosomes: current perspectives. Proteomics. 2008;8(19):4083–4099.

[3] Alderton G. Clinical uses of cellular communication. American Association for the Advancement of Science; 2020.

[4] Yurtsever A, Yoshida T, Behjat AB, Araki Y, Hanayama R, Fukuma T. Structural and mechanical characteristics of exosomes from osteosarcoma cells explored by 3D-atomic force microscopy. Nanoscale. 2021;13(13):6661–6677.

[5] Wu PH, Aroush DRB, Asnacios A, Chen WC, Dokukin ME, Doss BL, et al. A comparison of methods to assess cell mechanical properties. Nature methods. 2018;15:491–498.

[6] JPK Instruments Determining the elastic modulus of biological samples using atomic force microscopy;. Accessed: 2020-07-09. `https://www.jpk.com/app-technotes-img/AFM/pdf/jpk-app-elastic-modulus.14-1.pdf`.

[7] Wang ZL. Progress in piezotronics and piezo-phototronics. Advanced Materials. 2012;24(34):4632–4646.

[8] Zhang Y, Fang Y, Zhou X, Dong X. Image-based hysteresis modeling and compensation for an AFM piezo-scanner. Asian Journal of Control. 2009;11(2):166–174.

[9] Fronczek D, Quammen C, Wang H, Kisker C, Superfine R, Taylor R, et al. High accuracy FIONA–AFM hybrid imaging. Ultramicroscopy. 2011;111(5):350–355.

[10] The application of vsi (vertical scanning interferometry);. Accessed: 2020-07-11. `https://www.jobilize.com/nanotechnology/test/atomic-force-microscopy-the-application-of-vsi-vertical-by-openstax`.

[11] Gates RS, Pratt JR. Accurate and precise calibration of AFM cantilever spring constants using laser Doppler vibrometry. Nanotechnology. 2012;23(37):375702.

[12] Elasticity;. Accessed: 2020-07-10. `https://www.feynmanlectures.caltech.edu/II_38.html`.

[13] Hooke R. Lectures de potentia restitutiva, or, Of spring: Explaining the power of springing bodies : to which are added some collections. London: Printed for J. Martyn; 1678.

[14] Newton I. Principia mathematica. Book III, Lemma V, Case. 1934;1:1687.

[15] Ku HH, et al. Notes on the use of propagation of error formulas. Journal of Research of the National Bureau of Standards. 1966;70(4):263–273.

Appendix

A Force-displacement Plot for the Spring

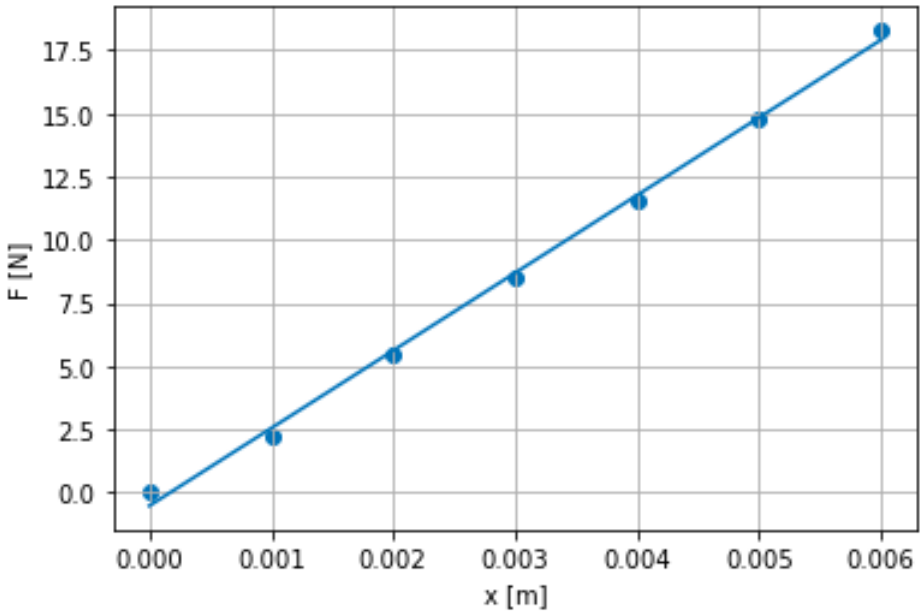

Figure 10: A straight line fitted to the data points obtained when the force acting on the spring, F, was plotted as a function of the compression of the spring x. The equation of the line is $F = 3000x - 0.50$. According to equation (3), the slope of this line corresponds to the spring constant of the spring.

B Plots for the Measurements on the Balloons

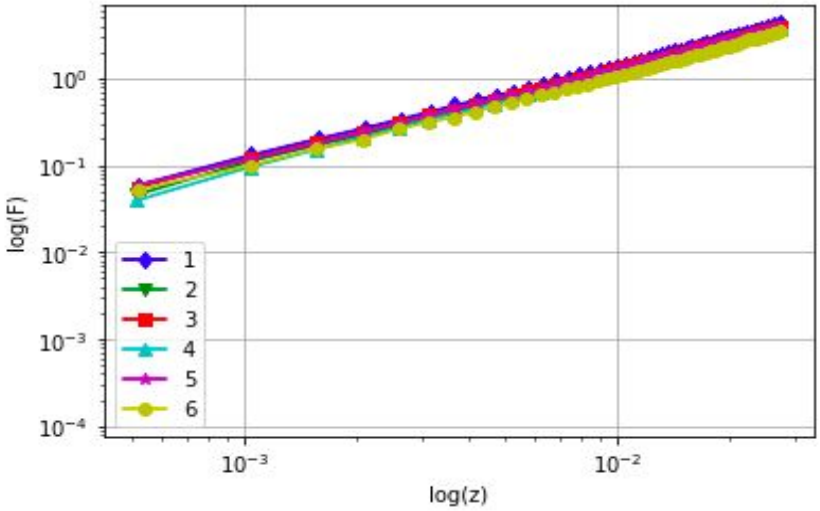

Figure 11: $\log(F)$ plotted as a function of $\log(z)$. The numbers in the legend correspond to the measurement numbers presented in table 1. The equations for lines 1 to 6 are $\log(F) = 1.07 \cdot \log(z) + 2.29$, $\log(F) = 1.10 \cdot \log(z) + 2.29$, $\log(F) = 1.07 \cdot \log(z) + 2.25$, $\log(F) = 1.12 \cdot \log(z) + 2.32$, $\log(F) = 1.08 \cdot \log(z) + 2.28$ and $\log(F) = 1.08 \cdot \log(z) + 2.21$.

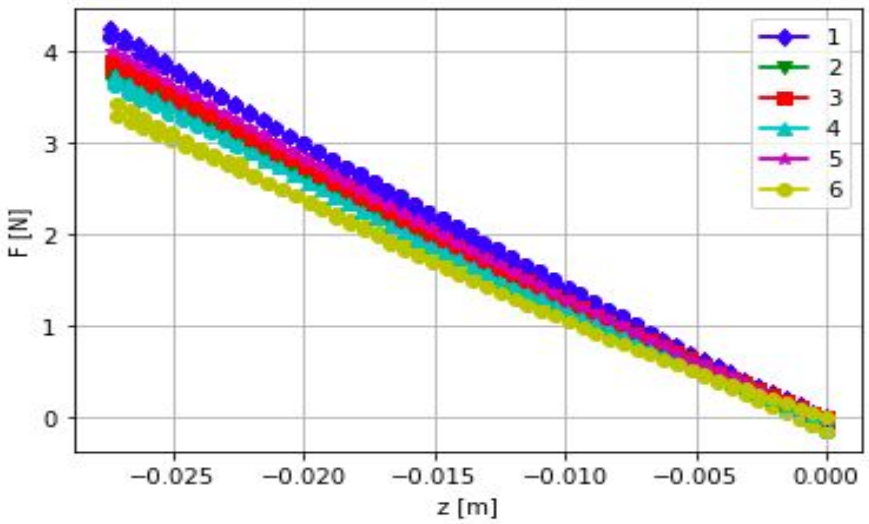

Figure 12: F plotted as a function of z. The numbers in the legend correspond to the measurement numbers presented in table 1. The equations for lines 1 to 6 are $F = -156z - 0.120$ $F = -142z - 0.140$, $F = -143z - 0.110$, $F = -138z - 0.150$, $F = -148z - 0.130$ and $F = -127z - 0.140$.

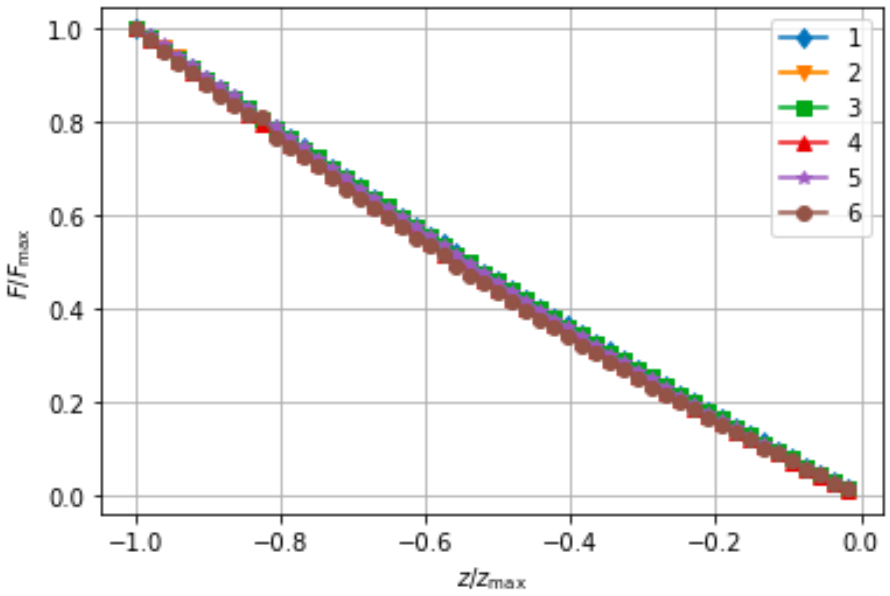

Figure 13: F divided by the maximal force acting on the balloon as a function of z divided by the maximal displacement of the balloon.